Materials Chemistry Horizons RESEARCH

Investigation of Protein-Ligand Interaction Using an Intermolecular Distance-Based Descriptor in Molecular Docking

Sarah Sadeghi [a], and Morteza Atabati [a,*]

[a] School of Chemistry, Damghan University, Damghan, Iran

***Corresponding author**: atabati@du.ac.ir (M. Atabati)

Mater. Chem. Horizons, 2025, 4(1), 59-76 10.22128/mch.2026.3086.1071 OPEN ACCESS

ABSTRACT

Molecular docking is a key tool in structure-based drug design, extensively used to study biomolecular interactions and mechanisms. Molecular docking reliability is often evaluated using RMSD (Root Mean Square Deviation) compared to experimental structures, though such data is frequently unavailable in practice. Therefore, scoring functions can be used as an alternative to assess protein-ligand docking results. In this study, a simple computational scoring function for protein-ligand interaction was developed, based on calculating the sum of pairwise distances between ligand atoms bound in the active site and protein atoms. The distance matrix can be used to calculate a distance-based score (DB-Score). To better evaluate performance, we used experimentally determined values for GRK6 (G protein-coupled receptor kinase 6) inhibitors to assess scoring and ranking accuracy compared to the AutoDock Vina program performances. Extensive experiments on this dataset demonstrate that the distance-based scoring function outperforms the conventional AutoDock Vina score in ranking and scoring. Pearson's correlation coefficients for AutoDock Vina and our defined score against experimentally determined GRK6- were 0.09 and 0.76, respectively. Furthermore, the effectiveness of DB-Score was evaluated using the v2016-core subset of the PDBbind database. On the CASF-2016 benchmark, DB-Score achieved a Pearson's r of 0.62, demonstrating surprisingly good performance.

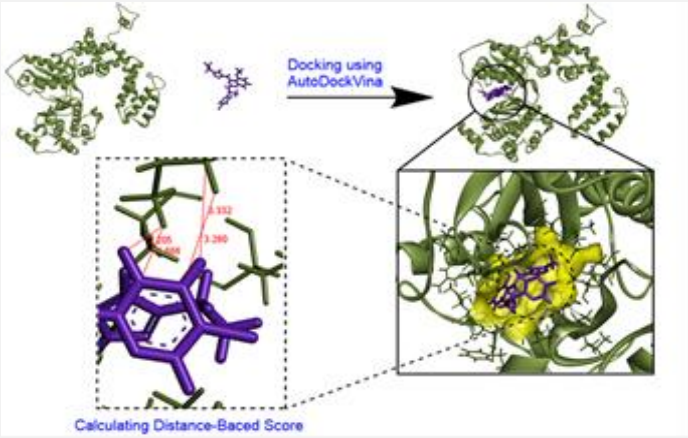

Keywords: Molecular docking, distance-based score, structure-based drug design, protein-ligand interaction, scoring function

1. Introduction

Molecular docking is one of the most widely used computer-aided drug design tools, simulating molecular interactions between small-molecule ligands and macromolecular targets to predict binding modes and affinities. [1-3]. Since the mid-1980s, molecular docking- alongside advances in chemistry, physics, biochemistry, and information technology- has become a cornerstone of drug discovery [4-6]. Computer-aided drug design tools for virtual screening and structure-based design are used in the industrial and academic drug discovery process daily [7-9]. Molecular docking is employed to estimate the binding affinity and dominant binding mode(s) of a ligand when it binds to a macromolecule with a known three-dimensional structure.

The primary explanation for the ligand-receptor binding mechanism, proposed by Fischer, is the lock-and-key theory, where the proper key (ligand) contains the appropriate pattern (conformation) to fit into a lock (receptor active site) [10]. The earliest proposed docking methods were based on Fisher's theory, in which both receptor and ligand were considered as rigid bodies [4]. The induced fit theory expanded the lock-and-key model, emphasizing that ligand binding reshapes the protein's active site during interaction [11]. Accordingly, it is better to consider ligands and receptors as flexible during docking [12]. Due to computer resource limitations, docking with a flexible

Received: October 08, 2025
Received in revised: November 01, 2025
Accepted: November 20, 2025

ligand and a rigid acceptor has long been the most common approach, and it remains prevalent today [13, 14]. There are two main types of computational strategies widely used for assessing the binding affinity of protein-ligand complexes. One type, which is also computationally expensive, is based on molecular dynamics simulations. These methods, widely applied in lead optimization and post-docking analysis, include computational approaches such as ASIE [15, 16], MM/GBSA-PBSA [17,18], and FEP/MD [19-21]. Another widely used approach in the rapid virtual screening of large chemical libraries is the scoring function (SF). The scoring function generally performs calculations based on only one spatial orientation of the protein-ligand structure, which is significantly faster.

To prioritize potentially favourable binding modes, molecular docking algorithms incorporate scoring functions, mathematical expressions designed to evaluate and rank the resulting docked poses based on their estimated binding affinity. These functions help to distinguish between non-binders and binders from the expansive number of docked compounds created in a single docking run. Various kinds of protein-ligand scoring functions have been developed over time, which fall under four broad classifications, including force field-based, knowledge-based, empirical, and machine learning-based SFs [22,23]. The continuous development and benchmarking of these diverse scoring approaches, particularly with the rise of machine learning, remain a central and rapidly evolving focus in computational chemistry to improve their predictive power and reliability [24, 25].

Despite advancements in scoring function development, persistent limitations in accuracy remain a primary bottleneck for reliable computational prediction of protein-ligand binding affinity [22, 26]. Therefore, ongoing refinement of robust scoring functions remains critical in the current situation. Scoring functions commonly applied in docking programs make many simplifications and assumptions to enable a more computationally efficient evaluation of ligand affinity. Naturally, the more accuracy is maintained against those simplifications, the more efficient that scoring function will be [22]. This challenge is further underscored by the rapid emergence of deep learning and artificial intelligence methods, which are creating new paradigms for predicting molecular interactions and pose ranking, yet often at the cost of interpretability and computational transparency [27, 28].

paper, we propose a simple computational distance-based scoring function, which is based on intermolecular distances between ligand and protein atoms. The distance matrix can be used to calculate distance-based scores. The use of geometric features, such as intermolecular distances and contact counts, has a precedent in the development of knowledge-based and other types of scoring functions [29-31]. However, the exploration of minimalist, geometry-based metrics as standalone scoring functions continues to be an area of interest for pose prediction and affinity ranking [32]. In this landscape, our DB-Score represents a deliberate pursuit of simplicity, interpretability, and computational transparency. While the use of a distance-sum may seem counter-intuitive to energy-based scoring principles, we posit it serves as a potent geometric proxy. A higher score indicates a greater number of ligand atoms situated within a close-contact shell of the protein. This implicitly reflects superior surface complementarity and a higher count of favourable van der Waals interactions, bypassing potential errors associated with the parameterization of specific energy terms in conventional functions. It serves as a robust, physics-inspired baseline that complements the growing complexity of AI-driven models ,providing immediate, practical utility where computational resources or interpretability are paramount [33, 34].

The model is trained on data including experimentally determined 40 inhibitors of G protein-coupled receptor kinase 6 (GRK6), serving as the essential kinase necessary for the viability of multiple myeloma (MM) cells, retrieved from the Uehling et al. study [35]. While significant advancements have been made in characterizing small-molecule interactions with GRK proteins, before the survey by Uehling et al. (2020), no dedicated publications existed on GRK6 inhibitors, and only a limited number of GRK6 ligands had been structurally characterized [36, 37]. Given the strong rationale for targeting GRK6 in MM, we sought to analyse better and investigate these novel GRK6 inhibitors through our computational approach. Benchmarking on the test set demonstrated that the proposed scoring function outperforms AutoDock Vina in both ranking and scoring accuracy.

2. Materials and methods

2.1. Preparation of structures

The crystal structure of the human G Protein-Coupled Receptor Kinase 6 (GRK6) in Complex with Sangivamycin (PDB ID: 3NYN) was retrieved from the Protein Data Bank database (PDB), which was obtained by X-ray diffraction method with 2.72 Å resolution [36]. The protein structure comprises two complete chains (A and B) with full residue coverage, as resolved in the deposited PDB entry. GRK6 targets that are used in this study were 40 small ligand molecules retrieved from the Uehling et al. study [35]. Two ligands (n1 and n2) were sourced from the PubChem Database [38], while the 2D structures of 38 additional ligands (n3–n40) were generated using ChemDraw Ultra 16.0 (PerkinElmer) [39]. **Figure 1** shows all the 2D structures of these GRK6 inhibitors.

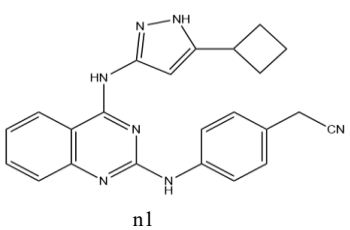

n1
pIC_{50} = 6.64

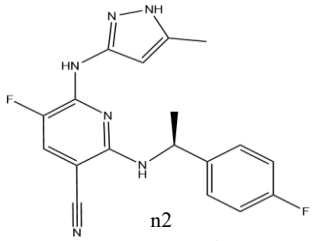

n2
pIC_{50} = 6.35

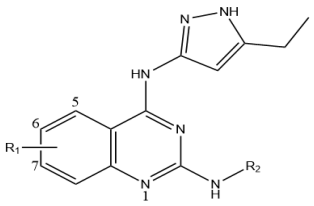

n3-n28

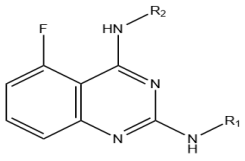

n29-n32

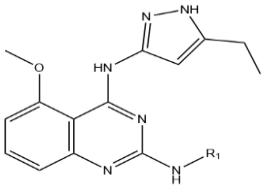

n33-n38

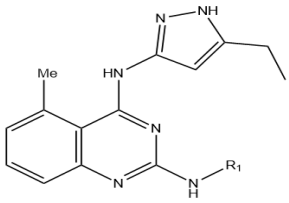

n39, n40

n3
pIC_{50} = 6.92
R_1=H
R_2=

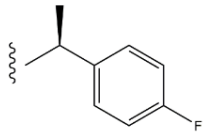

n4
pIC_{50} = 6.72
R_1=H
R_2=

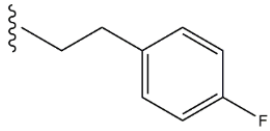

n5
pIC_{50} = 6.75
R_1=7-F
R_2=

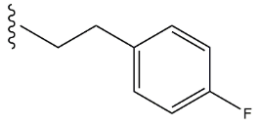

n6
pIC_{50} = 5.96
R_1=7-Cl
R_2=

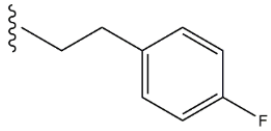

n7
pIC_{50} = 6.51
R_1=6-F
R_2=

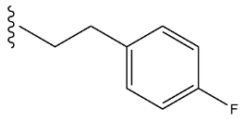

n8
pIC_{50} = 6.34
R_1=6-OMe
R_2=

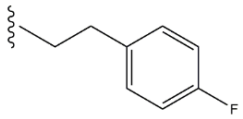

n9
pIC_{50} = 6.96
R_1=5-F
R_2=

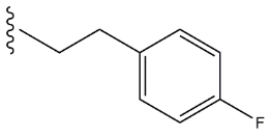

n10
pIC_{50} = 7.70
R_1=5-F
R_2=

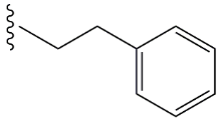

n11
pIC_{50} = 7.75
R_1=5-OMe
R_2=

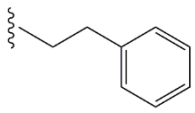

n12
pIC_{50} = 7.00
R_1=7-F
R_2=

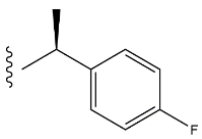

n13
pIC_{50} = 6.80
R_1=6-F
R_2=

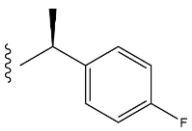

n14
pIC_{50} = 6.36
R_1=7-Cl
R_2=

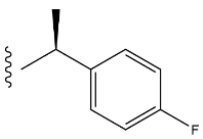

n15
pIC_{50} = 6.85
R_1=6-OMe
R_2=

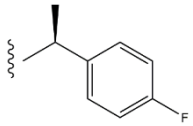

n16
pIC_{50} = 7.39
R_1=5-F
R_2=

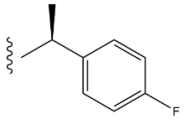

n17
pIC_{50} = 6.60
R_1= H
R_2=

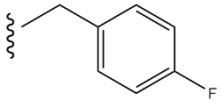

n18
pIC_{50} = 5.85
R_1= H
R_2=

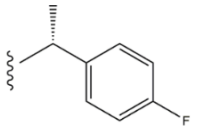

n19
pIC_{50} = 6.47
R_1= H
R_2=

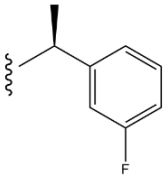

n20
pIC_{50} = 6.54
R_1= H
R_2=

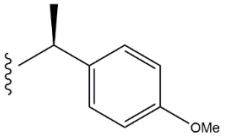

n21
pIC_{50} = 7.16
R_1= H
R_2=

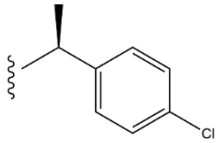

n22
pIC_{50} = 6.55
R_1= H
R_2=

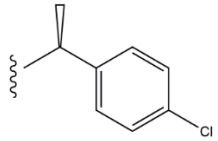

n23
pIC_{50} = 7.57
R_1= 5-F
R_2=

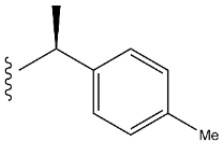

n24
pIC_{50} = 7.54
R_1= 5-F
R_2=

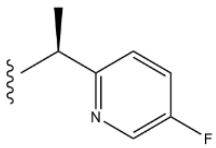

n25
pIC_{50} = 7.04
R_1= 5-F
R_2=

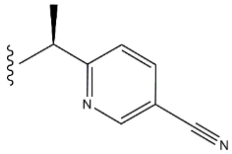

n26
pIC_{50} = 6.64
R_1=5-F
R_2=

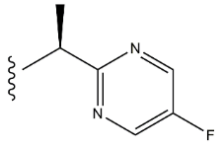

n27
pIC_{50} = 7.40
R_1= H
R_2=

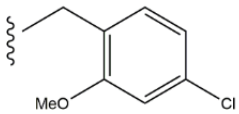

n28
pIC_{50} = 6.02
R_1= H
R_2=

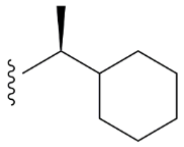

n29
pIC_{50} = 5.60
R_1= R_2=

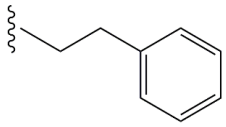

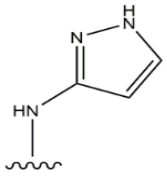

n30
pIC_{50} = 5.00
R_1= R_2=

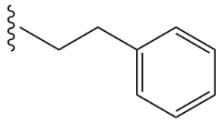

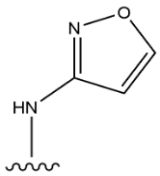

n31
pIC_{50} = 6.55
R_1= R_2=

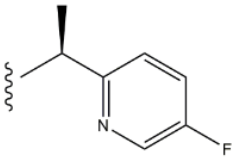

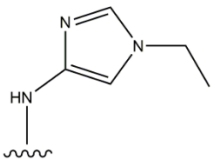

n32
pIC_{50} = 5.00
R_1= R_2=

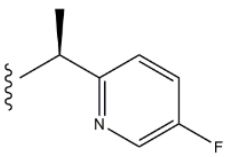

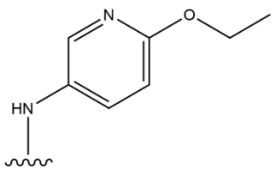

n33
pIC_{50} = 8.14
R_1=

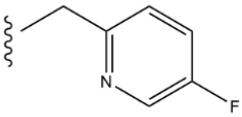

n34
pIC_{50} = 7.75
R_1=

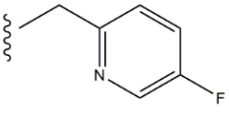

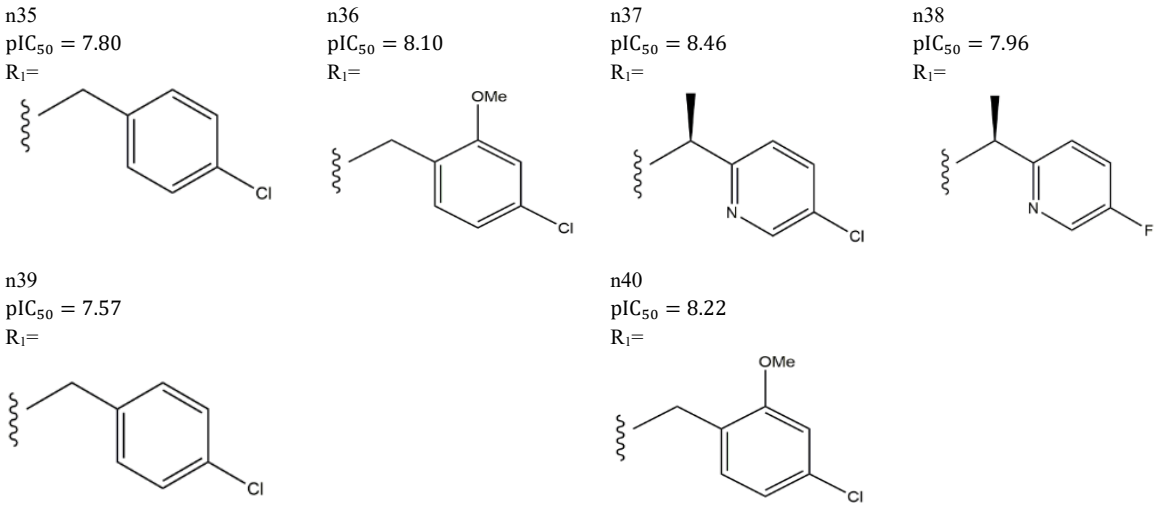

Figure 1. Structure of GRK6 inhibitors.

The structures of all 40 ligands were geometrically optimized using HyperChem 8.0 via semi-empirical methods with the Polack-Ribere algorithm for energy minimization. This approach was selected to generate high-quality, energetically minimized 3D starting structures for docking in a computationally feasible manner for our ligand dataset. While, higher-level methods like density functional theory (DFT) provide higher accuracy, they are computationally more demanding. Semi-empirical methods offer a practical compromise for pre-docking conformational optimization of a set of ligands of this size, giving reasonable geometries at a fraction of the computational cost, which is suitable for high-throughput docking workflows [40]. Additionally, Open Babel software was used for converting the different formats of ligand, protein, or protein-ligand complex structures [41].

2.2. Molecular docking

Molecular docking analysis was performed by AutoDock vina [42] to identify binding affinity and possible binding poses between GRK6 and ligand targets. The macromolecule was prepared in Discovery Studio 21.1 by removing chain B, solvent molecules, and non-essential heteroatoms. Subsequent charge assignment and docking preparation were performed in UCSF Chimera 1.15. Afterward, the collected PDB format files of ligands and protein were uploaded into Autodock Tools 1.5.6 [43]. All input files (protein receptor and ligand) were prepared in AutoDock Tools 1.5.6 and saved in PDBQT format for molecular docking via AutoDock Vina 1.1.2 [42]. Eventually, docking procedures between ligand and macromolecule were carried out via AutoDock Vina 1.1.2 using default parameters and an inner docking box size of 18×22×20 (**Figure 2**).

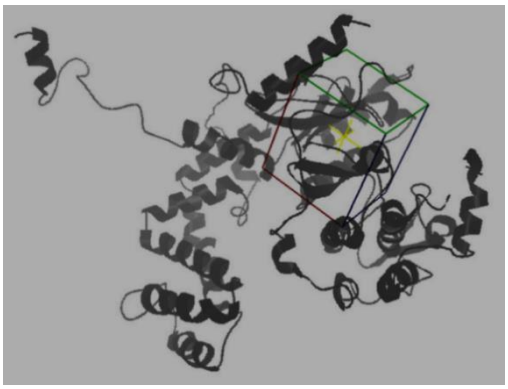

Figure 2. Docking grid box generating in AutoDock Tools.

The default AutoDock Vina output includes nine docking poses, with Pose 1 selected as the top-ranked solution based on minimized free-energy and structural alignment to the experimental binding mode (RMSD= 0). A lower binding energy score indicates a greater affinity between the ligand and the target macromolecules [44]. Moreover, the other eight modes were sorted by their affinity values, and also the RMSD lower bound (*rmsd* l.b.) and upper bound (*rmsd* u.b.) values were reported based on distances of each ligand docking pose from the best mode docking pose. The output of software for n37 is shown in **Figure 3.**

mode	affinity (kcal/mol)	dist from best mode rmsd l.b.	rmsd u.b.
1 Best mode	-9.3	0.000	0.000
2	-8.9	2.277	2.927
3	-8.9	1.868	2.496
4	-8.9	1.678	2.024
5	-8.9	2.886	6.490
6	-8.8	3.097	6.240
7	-8.7	3.547	6.958
8	-8.4	3.954	8.708
9	-8.3	3.712	7.125

Figure 3. The output of AutoDock Vina for n37, the best mode is mode 1 with *rmsd*= 0

For structural bioinformatics applications, the root-mean-square deviation (RMSD) is the principal algorithm for assessing conformational overlap between superimposed atomic models, with values conventionally expressed in angstroms (Å) and calculated as follows.

$$RMSD = \sqrt{\frac{1}{n}\sum_{i=1}^{n} d_i^2} \quad (1)$$

where the summation averages the squared distances (d_i^2) over n pairs of equivalent atoms, with d_i representing the displacement between the atomic coordinates of the i-th pair. The RMSD upper bound (u.b.) quantifies geometric similarity between two ligand conformations by superimposing corresponding atoms in a 1:1 pairwise manner, effectively measuring the structural conservation of all atomic positions. However, the RMSD lower bound (l.b.) will give you the best RMSD independent of atom numbering. Therefore, if there is any internal symmetry in ligands, *rmsd* l.b. provides a better ranking of docking results.

Since RMSD values provide a spatial metric for quantifying deviations between docked ligand poses, we ranked the output based on *rmsd* l.b. criteria, designating poses 2–9 as decoys due to their higher RMSD thresholds. Following the *rmsd* l.b. ranking, the first non-native mode (Pose 2) was defined as Decoy-1, and the final mode (Pose 9) was assigned as Decoy-8 for DB-Score validation, ensuring systematic evaluation of scoring function robustness (**Figure 4**). The generated PDB files of docked conformations were visualized in Discovery Studio 21.1 for structural analysis.

mode	affinity (kcal/mol)	dist from best mode rmsd l.b.	rmsd u.b.
1	-9.3	0.000	0.000
4 Decoy-1	-8.9	1.678	2.024
3	-8.9	1.868	2.496
2	-8.9	2.277	2.927
6	-8.8	3.097	6.240
5	-8.9	2.886	6.490
7	-8.7	3.547	6.958
9	-8.3	3.712	7.125
8 Decoy-8	-8.4	3.954	8.708

Figure 4. Sorted Output of AutoDock Vina for n37 by the RMSD lower bound (*rmsd* l.b.) values.

2.3. Calculating the distance-based score

To calculate the DB-Score, a program was written in MATLAB 2021 and applied in different steps. First, the spatial coordinates of all ligand atoms and the spatial coordinates of protein atoms were considered. Then, the sum of the distance between all the docked ligand atoms and all the protein atoms with 3 Å (d_{cutoff}) distances from them was obtained. It should be noted that d_{cutoff} was calculated without taking into account the atomic radii of ligand and protein atoms. In other words, the distance between atom pairs was selected based on the distance between their electron clouds. The total distance was calculated by summing up the distances between every atom of the docked ligand and every protein atom within a 3 Å (d_{cutoff}) distance from it. This obtained value was considered as a Distance-based score. The workflow for calculating the DB-Score is shown in **Figure 5.**

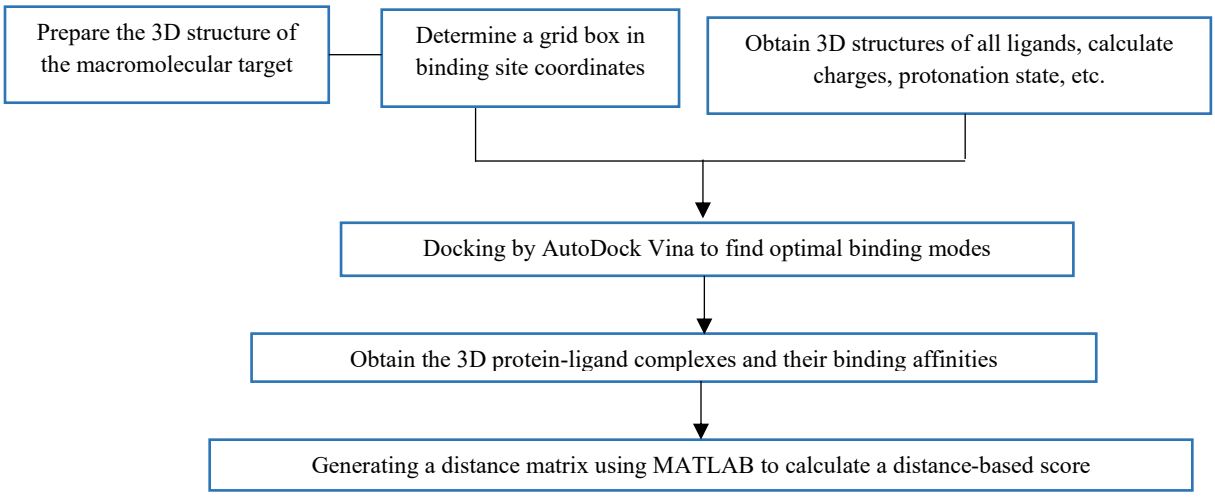

Figure 5. Schematic workflow for calculating DB-Score.

The relationship between the cutoff distance and the Pearson's correlation coefficient for the GRK6 dataset is illustrated in **Figure 6a**. The optimal cutoff was determined to be 3.0 Å, as it yielded the highest correlation with experimental pIC_{50} values. This distance is physically intuitive, corresponding to the typical range of strong van der Waals interactions and hydrogen bonds, ensuring the descriptor captures specific, short-range contacts at the binding interface. This parameter, identified from the GRK6 set, was subsequently applied without change to all external validation sets (CASF-2016 and BACE-1) to ensure an unbiased assessment of performance (**Figure 6b** and **c**).

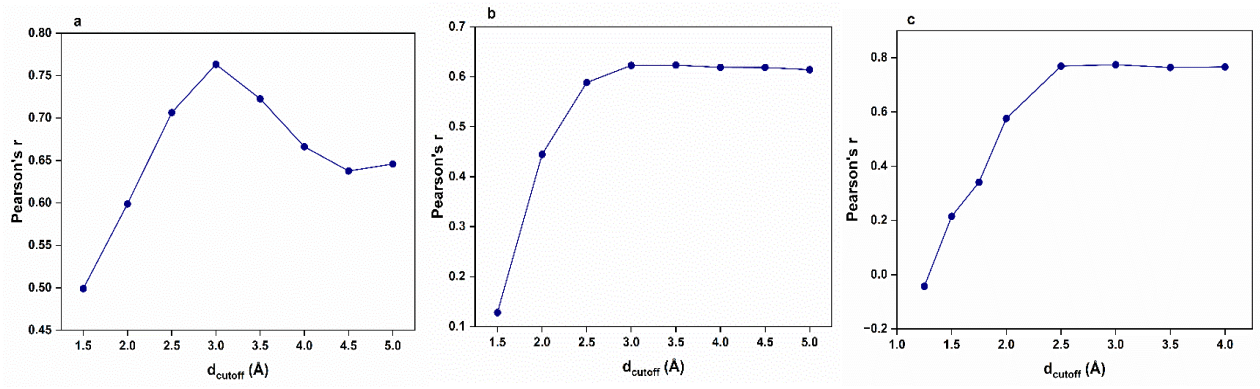

Figure 6. The optimization of the cutoff distance with the corresponding Pearson's correlation coefficient values for all three data sets (a) n=40, (b) n=285, and (c) n=91 data sets.

In general, scores obtained by docking programs could be evaluated by several metrics [24]. For this, all AutoDock Vina scores and distance-based scores were consequently tested regarding scoring power and ranking power. The basic principles and evaluation techniques for these metrics are explained subsequently.

2.4. Evaluating the scoring power

Scoring power is defined as the correlation between the binding scores predicted by a scoring function and the experimentally determined binding affinities for a series of protein-ligand complexes. [45]. Scoring power is quantified using Pearson's correlation coefficient (r), calculated as follows

$$r = \frac{\sum_i^n (x_i-\bar{x})(y_i-\bar{y})}{\sqrt{\sum_i^n (x_i-\bar{x})^2}\sqrt{\sum_i^n (y_i-\bar{y})^2}} \quad (2)$$

where x_i is the calculated distance-based score and y_i is the negative base-10 logarithm of experimental Half-maximal inhibitory concentration (pIC_{50}) of the *i*-th complex. Additionally, $\bar{x}$ and $\bar{y}$ denote the mean values of the computationally predicted scores and experimentally measured pIC_{50}values, respectively.

2.5. Evaluating the ranking power

The capacity of a scoring function to accurately estimate the binding affinity order among known ligands for a specific target protein is referred to as ranking power or relative ranking prediction [45]. One can use Spearman's rank correlation coefficient (ρ) or Kendall's rank correlation coefficient (τ) as an indicator to evaluate the ranking power quantitatively [24]. The following equation shows how to calculate Spearman's rank correlation coefficient [46].

$$\rho = \frac{\sum_i^n (rx_i-\overline{rx})(ry_i-\overline{ry})}{\sqrt{\sum_i^n (x_i-\overline{rx})^2}\sqrt{\sum_i^n (y_i-\overline{ry})^2}} \quad (3)$$

Here, rx_i and ry_i are the rank of the distance-based score and the rank of the negative base-10 logarithm of experimental Half-maximal inhibitory concentration of the *i-th* complex, respectively; n denotes the total number of samples. Kendall's rank correlation coefficient, τ, is defined according to the following formula [47]

$$\tau = \frac{n_c-n_d}{\sqrt{(n_c+n_d+T)(n_c+n_d+U)}} \quad (4)$$

where n_d ($n_{discord}$) and n_c ($n_{concord}$) represent the counts of concordant and discordant pairs, respectively. A pair of observations (x_i,y_i) and (x_j,y_j) is termed concordant if the ordering of their scores is consistent across both variables- that is, $x_i>x_j$ and $y_i>y_j$ or $y_i<y_j$ and $x_i<x_j$. Conversely, the pair is discordant if the ranking is inconsistent- such as when $y_i<y_j$

and, $x_i > x_j$ or $y_i > y_j$ and $x_i < x_j$. In this context, x_i denotes the new score for sample *i*, and y_i corresponds to the negative base-10 logarithm of its experimentally determined half-maximal inhibitory concentration. The variables T and U denote the number of tied pairs in *x* and *y*, respectively. Notably, if both $x_i = x_j$ and $y_i = y_j$ simultaneously, the pair is excluded from the tie counts T and U. Using the evaluation methods described above, one can utilize molecular docking as a "reverse screening" tool, as identifying potential protein targets for a given small molecule based on docking score correlations [48-50].

2.6. Evaluating the DB-score using CASF-2016

A widely employed dataset to estimate the binding affinity of protein-ligand in molecular docking is the PDBbind dataset [84]. In this study, we used the latest available PDBbind core set for the scoring power test of DB-Score. This dataset is a strict subset of the CASF-2016 benchmark's refined set, which contains diverse protein-ligand complexes resolved with high-resolution X-ray diffraction data. The PDBbind core set (CASF-2016) encompasses 285 non-redundant protein-ligand complexes, categorized into 57 structurally diverse protein families with the highest quality. The binding affinities in the core set are expressed based on the negative logarithm value of the dissociation constant (K_d) or inhibition constant (K_i) (for both values, $-\log K_a$ is used in this report). In the PDBbind dataset, native ligand structures are archived in SDF/mol2 formats, while protein structures are stored as PDB files, enabling compatibility with molecular docking and visualization workflows.

To evaluate the DB-Score's scoring power, we first generated distance-based scores for 285 PDBbind complexes using MATLAB R2021b, then computed Pearson's (r) and Spearman's (ρ) correlation coefficients against experimentally determined binding affinities. To validate the scoring function performance, we used decoy ligands for all 285 proteins using decoy structure data existing in CASF-2016. For this, since each protein had a diverse set of decoys, we selected the worst decoy with the maximum RMSD.

3. Results and discussion

3.1. Evaluation results of scoring power

Our discussion commences with an analysis of the scoring power test, which embodies the scoring function's capacity to demonstrate a linear correlation between distance-based scores and experimentally determined data obtained from a series of protein-ligand complexes. Although this test was conducted on experimentally validated complex structures, it is critical to emphasize that scoring functions must predict binding affinities in real-world scenarios where resolved protein-ligand structures are unavailable. A scoring function that fails to generate physically reasonable predictions for known structures would lack practical utility.

The absolute value of binding scores calculated by AutoDock Vina software and the negative base-10 logarithm of experimental half-maximal inhibitory concentration (pIC_{50}) for each ligand are given in the Supplementary Information (**Table S1**). After performing AutoDock Vina docking for all ligand-protein complexes, we analysed the top three poses per complex to assess correlations between our distance-based binding scores and experimental GRK6 pIC_{50} values. As previously described, the three retained modes for each ligand include the best mode (native-like conformation), Decoy-1, and Decoy-8. To assess the scoring power of the DB-Score, we first computed the distance-based score for the best mode conformations using Matlab software. All calculated DB-Scores for the best mode of 40 protein-ligand complexes are shown in the Supplementary Information (**Table S1**). Pearson's correlation coefficient (r) between the AutoDock Vina score and DB-Score for the best docking mode against experimental GRK6 pIC_{50} values is presented in **Table 1**. Compared with the Pearson's correlation coefficient between the best mode of AutoDock Vina scores and GRK6 pIC_{50} values (r = 0.088) (**Figure 7a**), the performance of the DB-Score (r = 0.763) (**Figure 7b**) is still good.

Table 1. The values of r, and ρ for AutoDock Vina score and DB-Scores of the best modes versus GRK6

Scores	r	ρ	τ
AutoDock Vina score	0.088	0.024	0.018
DB-Score	0. 763	0. 697	0. 541

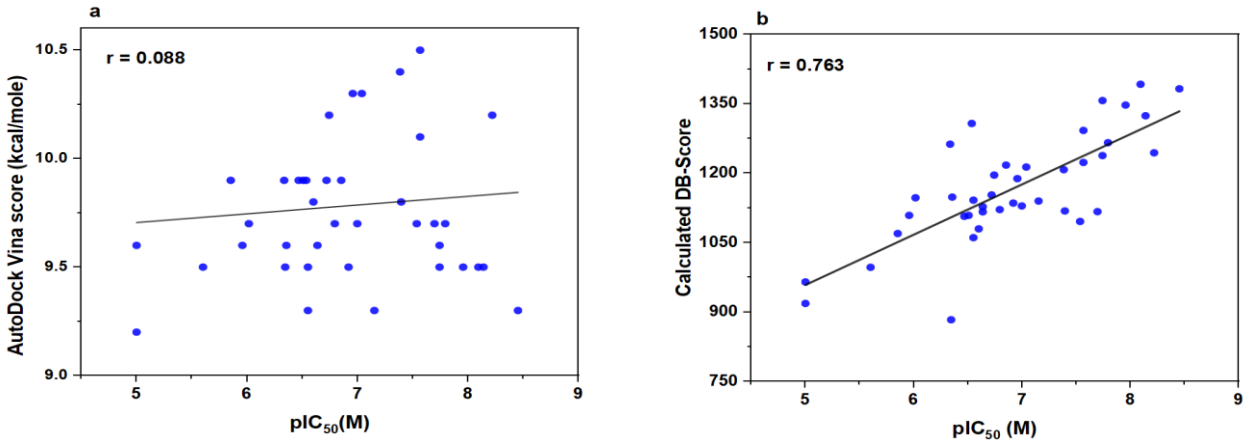

Figure 7. Assessing the (**a**) AutoDock Vina score and (**b**) the DB-Score for the best mode of 40 ligands versus pIC_{50} values.

To validate the assessment of the scoring power of the DB-Score, we computed the distance-based score for Decoy-1 and 8 conformations. Since the decoy structure of ligands has less interaction with the protein compared to the best mode, in calculating the DB-Score, it is expected that these scores, which are the sum of the distances between the individual ligand atoms and the protein atoms, will be lower. All calculated DB-Scores for two decoy conformations of 40 protein-ligand complexes are shown in the Supplementary Information (**Table S2**). It is assumed that the greater the interaction of the ligand with the protein, the more atoms situated within a distance of less than 3 Å from the protein atoms, which causes the DB-Score to have more values. For Decoy-1 and Decoy-8, the Pearson's *r* values between DB-Score and experimental GRK6 pIC_{50} were 0.342 and 0.232, respectively, indicating weak correlations (**Table S3**). As expected, Pearson's correlation coefficient values for decoys 1 and 8 have a downward trend compared to the best mode. Moreover, lower Pearson's correlation coefficients were obtained for Decoy-1 ($r = 0.342$) and Decoy-8 ($r = 0.232$) docking poses in protein-ligand complexes compared to the best mode Pearson's correlation coefficient value ($r = 0.763$), which indicates a logical relation for the best mode and the worst conformations (Decoy-8) of protein-ligand complexes (see **Figure 8**).

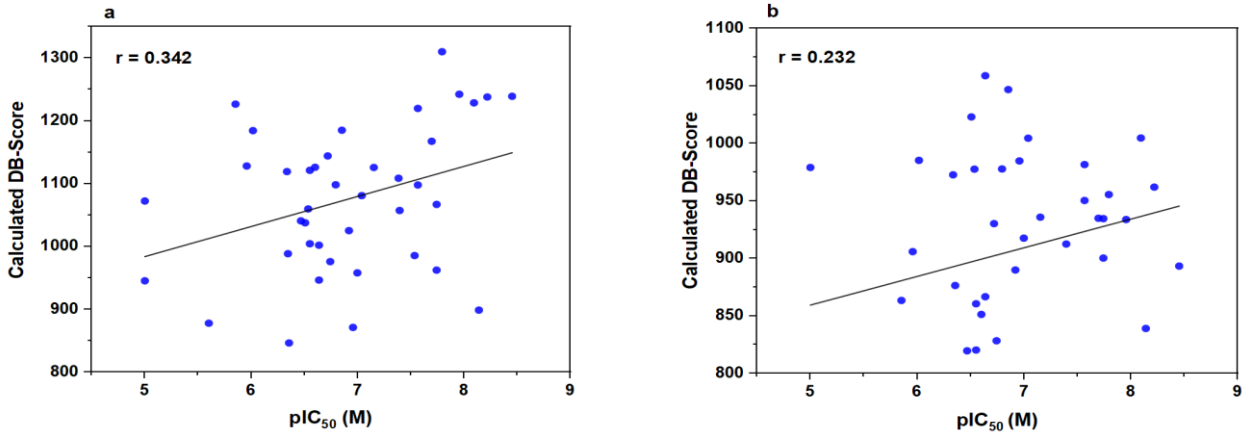

Figure 8. Performance of DB-Score for 40 ligand docking poses in GRK6; (**a**) Decoy-1, (**b**) Decoy-8.

3.2. Evaluation results of ranking power

As previously explained, either Spearman's correlation coefficient (ρ) or Kendall's correlation coefficient (τ) is utilized to assess the ranking power of a scoring function, which denotes its ability to rank distinct ligands against

a specific target accurately. The Spearman's rank correlation coefficients between AutoDock Vina scores and DB-Scores versus experimental GRK6 pIC_{50} values were 0.024 and 0.697, respectively (Table 1, Section 4.1). This demonstrates that DB-Score significantly outperforms the AutoDock Vina score. Additionally, the Spearman's rank correlation coefficients between DB-Scores for Decoy-1 (ρ = 0.310) and Decoy-8 (ρ = 0.192) and experimental GRK6 pIC_{50} values were significantly lower than those of the best mode (ρ = 0.697), confirming DB-Score's superior discriminative power for native-like poses (**Table S3**). Furthermore, Kendall's correlation coefficient (τ) between the DB-Scores of all three selected modes for all protein-ligand complexes, including the best mode, Decoy-1, and Decoy-8, and experimental GRK6 pIC_{50} were 0.541, 0.207, and 0.135, respectively, which shows the exact change as the Spearman's correlation coefficient values (see **Table S3**).

Evaluating the results obtained from the new computational distance-based score and the previously available experimental data shows that when the interaction between protein and ligand is greater, the calculated values for DB-Score will also be higher. The positive correlation between DB-Score and binding affinity can be interpreted as a geometric consequence of optimal binding. A stronger binder typically maximizes its contact with the protein surface, positioning more of its atoms within the interaction cutoff. This increases the total sum of distances. Furthermore, a higher sum suggests that these contacts are, on average, at the favorable outer range of the van der Waals potential, indicative of good steric fit without repulsive clashes, as opposed to a pose with fewer contacts or excessively short, strained distances. A stronger protein-ligand interaction or increased ligand activity for a specific protein correlates with a significant increase in the number of atomic contacts (distance < 3 Å) within the binding pose, as opposed to weaker interactions. To better clarify the DB-Score, some intermolecular distances for two Ligands (n32 and n37) and also their best mode docking poses with GRK6 are shown in **Figure 9.**

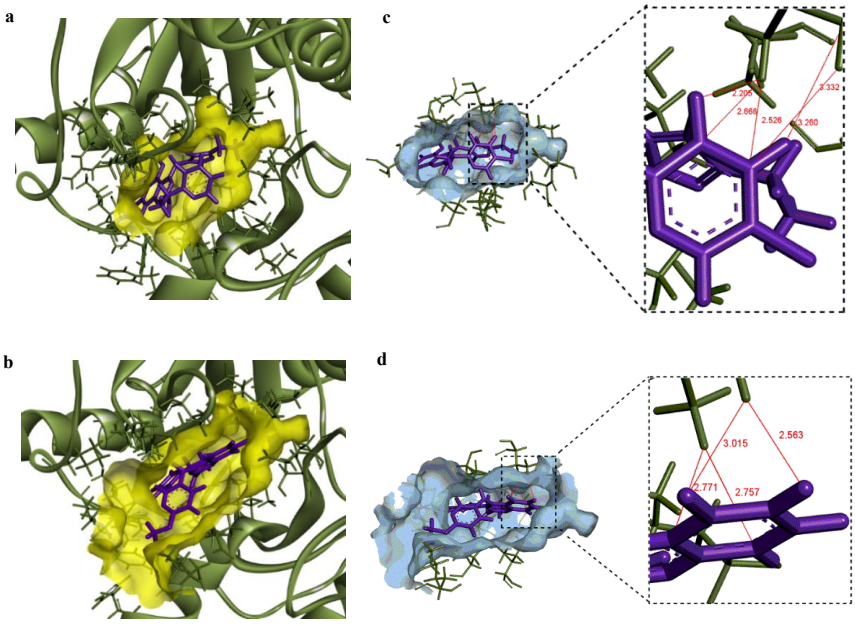

Figure 9. The conformation of the best (n37) **(a)** and the worst (n32) (**b)** inhibitor of GRK6 according to experimental pIC_{50} values in the protein active site after docking. Some intermolecular distances lower than 3 Å were demonstrated for n37 (**c)** and n32 (**d)** in the GRK6 active site.

3.3. Core set analysis

For assessing the scoring power of DB-Score, we used the CASF-2016 benchmark test. For this, the latest available core set (285 complexes) of the PDBbind database was used. To evaluate DB-Score's predictive power, we first calculated distance-based scores for all 285 protein-ligand complexes using MATLAB R2021b. All calculated DB-Score values for 285 protein-ligand complexes are shown in the Supplementary Information (**Table**

S4). As shown in **Figure 10a**, Pearson's correlation coefficient between experimental $-\log K_a$ values and calculated DB-Score was 0.623. Moreover, the Spearman's and Kendall's correlation coefficient between experimental $-\log K_a$ and calculated DB-Score were 0.613 and 0.441, respectively. This analysis demonstrates DB-Score's remarkable predictive efficacy across the full diversity of the PDBbind dataset (n = 285), despite its algorithmic simplicity. As explained before, all 285 protein-ligand complexes are clustered in 57 different protein families. In the per-cluster analysis case, the DB-Score can predict Pearson's correlation trend correctly within the majority of clusters (76% of all). For 67% of all clusters, the Pearson's r values exceeded 0.7, and for 9% of them, the values were between 0.6 and 0.7. To validate the scoring function's performance, we utilized decoy ligands with the maximum RMSD values from the CASF-2016 benchmark's decoy set (n = 285 proteins), ensuring robustness in distinguishing native-like poses from non-native conformations. All calculated DB-Score values for decoy conformation of 285 protein-ligand complexes are shown in the Supplementary Information (**Table S5**). As expected, lower Pearson's correlation coefficients (r = 0.335) were obtained in decoy analysis (see **Figure 10b**).

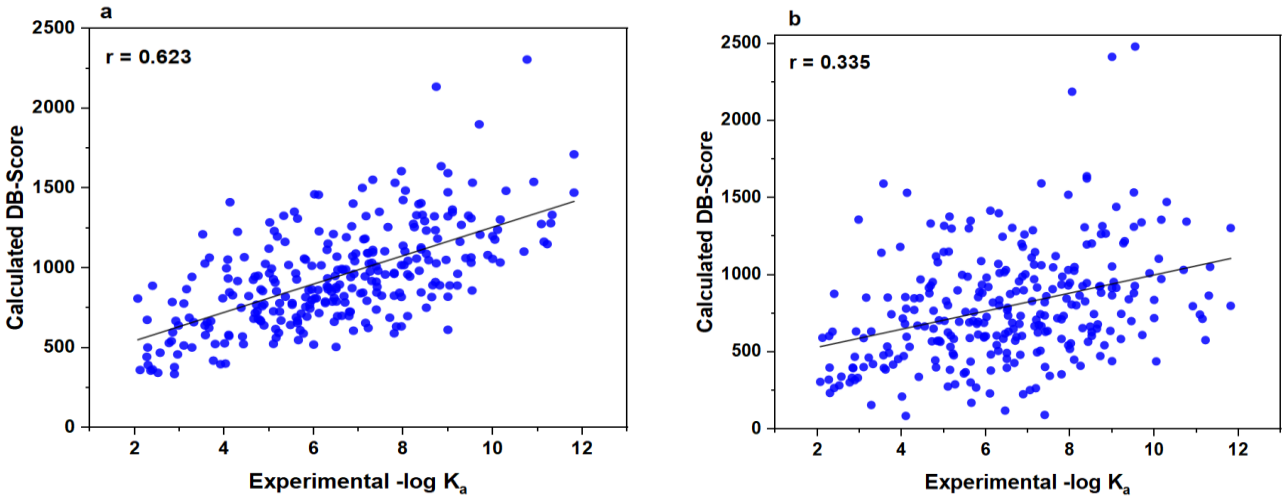

Figure 10. Performance of DB-Score for complexes from the v2016 core set (**a**) with native ligand (**b**) with the decoy.

3.4. Additional evaluations

To provide further insights into the performance of the distance-based score in specific categories of protein−ligand complexes, we conducted a re-evaluation of the DB-Score using three distinct sets of subsets derived from the core set of the PDBbind database. These subsets were analysed with respect to their scoring and ranking power. Each of the three subsets was constructed to reflect a shared physicochemical characteristic relevant to ligand–receptor interactions. Specifically, these characteristics include: the excluded volume within the binding site upon ligand association (denoted as ΔVOL), the percentage of solvent-accessible surface area (SAS) of the ligand that undergoes burial during binding (ΔSAS), and the hydrophobicity of the binding site, described by a hydrophobic scale (H-scale). Following the classification introduced by Su et al., the subsets categorized by ΔVOL are labeled V1, V2, and V3; those based on ΔSAS are designated as S1, S2, and S3; and the subsets defined by the H-scale are referred to as H1, H2, and H3, respectively [84].

The scoring and ranking performance of the DB-score across different subsets is presented in **Table S6**. The method demonstrates enhanced predictive capability for target proteins characterized by medium-sized binding pockets (subset V2, Pearson's r = 0.67) and for complexes in which the ligands exhibit higher solvent exposure (subset S1, Pearson's r = 0.75). These observations suggest that strain energy variations play a more prominent role when the ligand is not deeply embedded within the binding cavity. Moreover, the DB-score

also shows improved performance for targets with moderately hydrophobic binding sites (subset H2, Pearson's r = 0.71) (see **Table S6**). Additionally, the DB-Score's performance on a distinct biological target was assessed using Pearson's (r) and Spearman's (ρ) correlation coefficients, confirming its generalizability across protein families. In pursuit of this goal, we collected a test set comprising 91 complexes of β-Secretase 1 (BACE-1) (the detailed list of all the collected crystal complexes and calculated D-Score values is shown in **Table S7**). the Pearson and Spearman correlation coefficient between experimental data and calculated DB-Score were 0.774 and 0.719, respectively, demonstrating its surprisingly good performance (**Figure 11**).

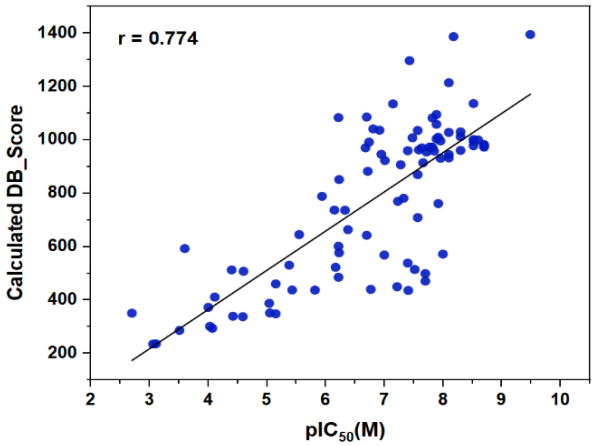

Figure 11. Assessing the DB-Score for BACE-1 complexes versus pIC_{50} values (n = 91).

3.5. Comparison with a simple contact count

To further elucidate the physical basis of the DB-Score, we investigated whether its performance was primarily driven by the number of contacts or the specific distance information. We calculated a simple geometric baseline: the count of protein-ligand atom pairs within the 3 Å cutoff (`COUNT`), and compared its correlation with experimental values to that of our distance-sum descriptor (`SUM`). For the GRK6 set, the `COUNT` metric achieved a Pearson's *r* of 0.764, virtually identical to the DB-Score (*r* = 0.763). This confirms that the fundamental predictive signal is the number of close intermolecular contacts, which serves as a robust geometric proxy for the burial of ligand surface area and the formation of favorable van der Waals interactions.

However, on the larger and more structurally diverse CASF-2016 and BACE-1 benchmarks, the `SUM` descriptor demonstrated a consistent, albeit slight, performance advantage (CASF-2016: `SUM` *r* = 0.623 vs. `COUNT` *r* = 0.617; BACE-1: `SUM` *r* = 0.774 vs. `COUNT` *r* = 0.772). We posit that this is because the `SUM` descriptor contains more nuanced information. While `COUNT` is a binary measure, the `SUM` descriptor implicitly weights contacts by their distance. A contact at 2.1 Å contributes less to the total sum than a contact at 2.9 Å. In physical terms, a larger sum indicates that, on average, the close contacts are at the outer, more favorable range of the van der Waals potential, potentially reflecting a less strained or more optimal interaction geometry. Therefore, we retained the sum of distances as the definition of the DB-Score, as it provides a marginally more discriminative and physically nuanced measure without adding algorithmic complexity.

3.6. Comparison with different scoring functions

Figure S1 in the Supplementary Information illustrates a comparison of scoring power between DB-Score (highlighted in black) and other scoring functions, as quantified by Pearson's correlation coefficient. According to the lower panel figure, one can see that all ML-based scoring functions (top 12 scoring functions) exhibit remarkable convergence in predictive performance for binding scores, with metric variations confined

to the second decimal place. This performance parity persists despite substantial variations in their underlying feature engineering approaches. Recent evaluations of machine-learning models using the CASF-2016 benchmark have demonstrated their superior performance relative to traditional scoring functions. While certain machine learning scoring functions exhibit superior performance under constrained experimental conditions, their reliance on training set size results in context-dependent accuracy across diverse biological systems.

Equally critical, however, direct comparisons between conventional scoring functions, our proposed DB-Score, and ML-based methods are methodologically biased due to differences in algorithmic complexity and training data requirements. Our proposed DB-Score employs a distance-based descriptor, eliminating the need for complex computations or high computational resources, while still yielding reliable predictions. As seen in the upper panel figure (**Figure S1**), DB-Score, compared to 34 conventional and standard scoring functions, stands in the top 5 rank. Surprisingly, it performs acceptably well relative to the simplicity of the method. All Pearson correlation coefficient values of different SFs are summarized in **Table S8**.

A compelling rationale for the DB-Score's strong performance may stem from its inherent robustness against the parameterization errors that can plague physics-based scoring functions. Traditional functions, such as those used in AutoDock Vina, rely on pre-defined force fields to decompose binding energy into distinct physical terms (e.g., van der Waals, hydrogen bonding, electrostatics). The accuracy of these functions is therefore fundamentally dependent on the quality and transferability of their underlying parameters. Any systematic bias or inaccuracy in these parameters—especially for less common chemical groups or metal ions—can propagate and lead to consistent mis-scoring of ligands containing those moieties. In stark contrast, the DB-Score is a purely geometric descriptor. It is agnostic to atom types, chemical functionalities, or the specific nature of the intermolecular interactions. By design, it circumvents the need for any force field parameters, relying instead on a simple, universal principle: the extent of close-range proximity between the ligand and the protein. This parameter-free nature makes the DB-Score a highly generalizable and robust tool. Its performance is less likely to be compromised by the specific chemical composition of the system under study, thereby offering a consistent and unbiased evaluation that is resilient to the particular errors inherent in more complex, physically-grounded models.

A second, more speculative but intriguing hypothesis is that the DB-Score may implicitly capture critical thermodynamic contributions, namely solvation and entropy, that are notoriously difficult to model explicitly. A high DB-Score, which signifies a ligand that achieves extensive close contacts, is effectively a measure of how well the ligand "fills" the binding pocket and achieves steric complementarity. This efficient pocket-filling inherently leads to the displacement of water molecules from the binding site. It is well-established that water molecules confined within protein pockets, particularly in hydrophobic environments, are often in a high-energy, entropically unfavorable state. The thermodynamic gain from releasing these ordered, energetically "unhappy" water molecules into the bulk solvent is a major driver of binding affinity. While many scoring functions treat solvation and entropic effects with crude, often inadequate empirical terms, the DB-Score may act as a powerful, albeit indirect, proxy for this phenomenon.

It is crucial to delineate the scope and limitations of the DB-Score. As a post-docking re-scoring function, it is not designed to predict absolute binding affinity nor replace the sampling and scoring steps of docking itself. Its application is to re-rank pre-generated poses from tools like AutoDock Vina to achieve a better correlation with experimental data. Furthermore, the DB-Score is inherently a steric and contact-based descriptor. It lacks explicit terms for key physicochemical interactions such as electrostatic contributions, explicit hydrogen bonding, desolvation penalties, or entropy. Its success implies that for many systems, especially those dominated by hydrophobic and van der Waals interactions, steric complementarity is a dominant and predictive factor. However, its performance may be less reliable for systems where electrostatics or specific, directional hydrogen bonds are the primary drivers of binding.

4. Conclusion

In this study, we introduced a simple computational protein-ligand scoring function based on the pairwise distances between ligand and protein atoms. To rigorously evaluate the performance of this distance-based scoring function, we employed a previously validated dataset containing experimentally measured GRK6 pIC50 values, enabling systematic assessment of scoring and ranking power compared to AutoDock Vina

program performances. Extensive experiments on this data revealed that the proposed scoring function significantly outperforms AutoDock Vina in both ranking and scoring. Validation via the CASF-2016 benchmark confirmed DB-Score's performance is surprisingly good. The enhanced performance of DB-Score is driven by its algorithmic simplicity and computational efficiency. Since in computer-aided drug discovery, predicting the exact binding pose of a ligand to its target protein and the corresponding binding affinity constitutes a pivotal challenge, we suppose that DB-Score can be applied successfully in this field. The success of the DB-Score is attributed to its role as a robust geometric proxy for the number and quality of close intermolecular contacts, a fundamental driver of binding affinity. Its transparency and computational efficiency stand in contrast to the "black box" nature of many modern machine-learning approaches, positioning it as a valuable, interpretable baseline for the field. Additionally, DB-Score was developed using MATLAB code,which can be easily embedded in other workflows. It is critical to note that DB-Score is applied post-docking, as conventional tools like AutoDock Vina lack robust correlations with experimental data, necessitating post-processing via our scoring function for reliable predictions. Therefore, our scoring function can be utilized to establish a stronger connection between the scores generated and experimental results. It should be noted that the score obtained from our scoring function cannot be used to compare structures with different RMSD values in the output of docking software such as AutoDock Vina, as this scoring function is not designed to predict protein-ligand binding affinity. Instead, this scoring function applies to post-docking operations to better correlate with experimental results. Therefore, screening power and docking power tests are not executable and evaluable in this method as the primary aim is not to estimate protein–ligand binding affinity. Unlike conventional docking workflows, our approach first identifies stable ligand conformations via AutoDock Vina, then re-ranks them using DB-Score to prioritize drug candidates. Therefore, it is recommended to use the introduced scoring function after molecular docking operations using software such as AutoDock Vina, as our scoring function can better correlate scores with experimental values in further steps.

Authors' contributions

All authors contributed equally to data curation, formal analysis, investigation, writing– original draft, and writing–review & editing. All authors have read and agreed to the published version of the manuscript.

Declaration of competing interest

The authors declare that they have no conflict of interest.

Funding

This paper received no funding.

Data availability

Data will be made available on request.

References

[1] S.-Y. Huang, X. Zou, Advances and challenges in protein-ligand docking, Int. J. Mol. Sci. 11 (2010) 3016-3034.
DOI: https://doi.org/10.3390/ijms11083016
[2] J. Fan, A. Fu, L. Zhang, Progress in molecular docking, Quant. Biol. 7 (2019) 83-89.
DOI: https://doi.org/10.1007/s40484-018-0163-4
[3] P.H. Torres, A.C. Sodero, P. Jofily, F.P. Silva-Jr, Key topics in molecular docking for drug design, Int. J. Mol. Sci. 20 (2019) 4574.
DOI: https://doi.org/10.3390/ijms20184574
[4] I.D. Kuntz, J.M. Blaney, S.J. Oatley, R. Langridge, T.E. Ferrin, A geometric approach to macromolecule-ligand interactions, J. Mol. Biol. 161 (1982) 269-288.
DOI: https://doi.org/10.1016/0022-2836(82)90153-X
[5] E. Lionta, G. Spyrou, D.K. Vassilatis, Z. Cournia, Structure-based virtual screening for drug discovery: principles, applications and recent advances, Curr. Top. Med. Chem. 14 (2014) 1923-1938.
DOI: https://doi.org/10.2174/1568026614666140929124445

[6] L.G. Ferreira, R.N. Dos Santos, G. Oliva, A.D. Andricopulo, Molecular docking and structure-based drug design strategies, Molecules 20 (2015) 13384-13421.
DOI: https://doi.org/10.3390/molecules200713384
[7] P. Śledź, A. Caflisch, Protein structure-based drug design: from docking to molecular dynamics, Curr. Opin. Struct. Biol. 48 (2018) 93-102.
DOI: https://doi.org/10.1016/j.sbi.2017.10.010
[8] X. Lin, X. Li, X. Lin, A review on applications of computational methods in drug screening and design, Molecules 25 (2020) 1375.
DOI: https://doi.org/10.3390/molecules25061375
[9] S.S. Bhunia, M. Saxena, A.K. Saxena, Ligand- and structure-based virtual screening in drug discovery, in: A. Saxena (Ed.), Biophysical and Computational Tools in Drug Discovery, Springer, Cham, 2021, pp. 281-339.
DOI: https://doi.org/10.1007/7355_2021_128
[10] G. Klebe, Protein–ligand interactions as the basis for drug action, in: Drug Design: From Structure and Mode-of-Action to Rational Design Concepts, Springer, Berlin, Heidelberg, 2025, pp. 39–65. ISBN: 978-3-662-70235-2 (eBook).
[11] D. Koshland, Jr., Correlation of Structure and Function in Enzyme Action: Theoretical and experimental tools are leading to correlations between enzyme structure and function, Science 142 (1963) 1533-1541.
DOI: https://doi.org/10.1126/science.142.3599.1533
[12] M. van den Noort, M. de Boer, B. Poolman, Stability of ligand-induced protein conformation influences affinity in maltose-binding protein, J. Mol. Biol. 433 (2021) 167036.
DOI: https://doi.org/10.1016/j.jmb.2021.167036
[13] V.B. Sulimov, D.C. Kutov, A.V. Sulimov, Advances in docking, Curr. Med. Chem. 26 (2019) 7555-7580.
DOI: https://doi.org/10.2174/0929867326666181203122542
[14] B. Waszkowycz, D.E. Clark, E. Gancia, Outstanding challenges in protein–ligand docking and structure-based virtual screening, Wiley Interdiscip. Rev. Comput. Mol. Sci. 1 (2011) 229-259.
DOI: https://doi.org/10.1002/wcms.18
[15] Y. Yan, M. Yang, C.G. Ji, J.Z. Zhang, Interaction entropy for computational alanine scanning, J. Chem. Inf. Model. 57 (2017) 1112-1122.
DOI: https://doi.org/10.1021/acs.jcim.7b00025
[16] X. Liu, L. Peng, Y. Zhou, Y. Zhang, J.Z. Zhang, Computational alanine scanning with interaction entropy for protein–ligand binding free energies, J. Chem. Theory. Comput. 14 (2018) 1772-1780.
DOI: https://doi.org/10.1021/acs.jctc.8b00026
[17] H. Sun, L. Duan, F. Chen, H. Liu, Z. Wang, P. Pan, F. Zhu, J.Z. Zhang, T. Hou, Assessing the performance of MM/PBSA and MM/GBSA methods. 7. Entropy effects on the performance of end-point binding free energy calculation approaches, Phys. Chem. Chem. Phys. 20 (2018) 14450-14460.
DOI: https://doi.org/10.1039/C7CP07623A
[18] E. Wang, H. Sun, J. Wang, Z. Wang, H. Liu, J.Z. Zhang, T. Hou, End-point binding free energy calculation with MM/PBSA and MM/GBSA: strategies and applications in drug design, Chem. Rev. 119 (2019) 9478-9508.
DOI: https://doi.org/10.1021/acs.chemrev.9b00055
[19] L. Wang, J. Chambers, R. Abel, Protein–ligand binding free energy calculations with FEP+, in: M. Bonomi, C. Camilloni (Eds.), Biomolecular Simulations: Methods and Protocols, Humana Press, New York, 2019, pp. 201-232.
DOI: https://doi.org/10.1007/978-1-4939-9608-7_9
[20] P.V. Rusina, I.Y. Titov, M.V. Panova, V.S. Stroylov, Y.R. Abdyusheva, E.Y. Murlatova, I.V. Svitanko, F.N. Novikov, Modeling of novel CDK7 inhibitors activity by molecular dynamics and free energy perturbation methods, Mendeleev Commun. 30 (2020) 430-432.
DOI: https://doi.org/10.1016/j.mencom.2020.07.002
[21] L.M. Mihalovits, G.G. Ferenczy, G.M. Keserű, Affinity and selectivity assessment of covalent inhibitors by free energy calculations, J. Chem. Inf. Model. 60 (2020) 6579-6594.
DOI: https://doi.org/10.1021/acs.jcim.0c01067
[22] J. Liu, R. Wang, Classification of current scoring functions, J. Chem. Inf. Model. 55 (2015) 475-482.
DOI: https://doi.org/10.1021/ci500731a
[23] J. Li, A. Fu, L. Zhang, An overview of scoring functions used for protein–ligand interactions in molecular docking, Interdiscip. Sci.: Comput. Life Sci. 11 (2019) 320–328.
DOI: https://doi.org/10.1007/s12539-019-00327-w
[24] M. Su, Q. Yang, Y. Du, G. Feng, Z. Liu, Y. Li, R. Wang, Comparative assessment of scoring functions: the CASF-2016 update, J. Chem. Inf. Model. 59 (2018) 895-913.
DOI: https://doi.org/10.1021/acs.jcim.8b00545
[25] O. Méndez-Lucio, M. Ahmad, E.A. del Rio-Chanona, J.K. Wegner, A geometric deep learning approach to predict binding conformations of bioactive molecules, Nat. Mach. Intell. 3 (2021) 1033-1039.
DOI: https://doi.org/10.1038/s42256-021-00409-9

[26] T. Harren, T. Gutermuth, C. Grebner, G. Hessler, M. Rarey, Modern machine-learning for binding affinity estimation of protein–ligand complexes: Progress, opportunities, and challenges, Wiley Interdiscip. Rev. Comput. Mol. Sci. 14 (2024) e1716. **DOI**: https://doi.org/10.1002/wcms.1716
[27] K. Abbasi, P. Razzaghi, A. Poso, S. Ghanbari-Ara, A. Masoudi-Nejad, Deep learning in drug target interaction prediction: current and future perspectives, Curr. Med. Chem. 28 (2021) 2100-2113. **DOI**: https://doi.org/10.2174/0929867327666200908145101
[28] D.P. Kiouri, G.C. Batsis, C.T. Chasapis, Structure-Based Approaches for Protein–Protein Interaction Prediction Using Machine Learning and Deep Learning, Biomolecules 15 (2025) 141. **DOI**: https://doi.org/10.3390/biom15010141
[29] R. Chen, Z. Weng, A novel shape complementarity scoring function for protein-protein docking, Proteins: Struct. Funct. Bioinf. 51 (2003) 397-408. **DOI**: https://doi.org/10.1002/prot.10334
[30] A. Shirali, V. Stebliankin, U. Karki, J. Shi, P. Chapagain, G. Narasimhan, A comprehensive survey of scoring functions for protein docking models, BMC Bioinf. 26 (2025) 25. **DOI**: https://doi.org/10.1186/s12859-024-05869-5
[31] D. Fischer, S.L. Lin, H.L. Wolfson, R. Nussinov, A geometry-based suite of molecular docking processes, J. Mol. Biol. 248 (1995) 459-477. **DOI**: https://doi.org/10.1006/jmbi.1995.0235
[32] J. Rahman, M.H. Newton, M.E. Ali, A. Sattar, Distance plus attention for binding affinity prediction, J. Cheminform. 16 (2024) 52. **DOI**: https://doi.org/10.1186/s13321-024-00854-9
[33] J. Gabel, J. Desaphy, D. Rognan, Beware of Machine Learning-Based Scoring Functions: On the Danger of Developing Black Boxes, J. Chem. Inf. Model. 54 (2014) 2807-2815. **DOI**: https://doi.org/10.1021/ci500406k
[34] C. Rudin, C. Chen, Z. Chen, H. Huang, L. Semenova, C. Zhong, Interpretable machine learning: Fundamental principles and 10 grand challenges, Stat. Surv. 16 (2022) 1-85. **DOI**: https://doi.org/10.1214/21-SS133
[35] D.E. Uehling, B. Joseph, K.C. Chung, A.X. Zhang, S. Ler, M.A. Prakesch, G. Poda, J. Grouleff, A. Aman, T. Kiyota, Design, synthesis, and characterization of 4-aminoquinazolines as potent inhibitors of the G protein-coupled receptor kinase 6 (GRK6) for the treatment of multiple myeloma, J. Med. Chem. 64 (2021) 11129-11147. **DOI**: https://doi.org/10.1021/acs.jmedchem.1c00192
[36] C.A. Boguth, P. Singh, C.C. Huang, J.J. Tesmer, Molecular basis for activation of G protein-coupled receptor kinases, EMBO J. 29 (2010) 3249-3259. **DOI**: https://doi.org/10.1038/emboj.2010.206
[37] K.T. Homan, J.J. Tesmer, Molecular basis for small molecule inhibition of G protein-coupled receptor kinases, ACS Chem. Biol. 10 (2015) 246-256. DOI: https://doi.org/10.1021/cb5003163
[38] S. Kim, J. Chen, T. Cheng, A. Gindulyte, J. He, S. He, Q. Li, B.A. Shoemaker, P.A. Thiessen, B. Yu, PubChem in 2021: new data content and improved web interfaces, Nucleic Acids Res. 49 (2021) D1388-D1395. **DOI**: https://doi.org/10.1093/nar/gkaa971
[39] D.A. Evans, History of the Harvard ChemDraw project, Angew. Chem. Int. Ed. Engl. 53 (2014) 11140-11145. **DOI**: https://doi.org/10.1002/anie.201405820
[40] J.J. Stewart, Optimization of parameters for semiempirical methods V: Modification of NDDO approximations and application to 70 elements, J. Mol. Model. 13 (2007) 1173-1213. **DOI**: https://doi.org/10.1007/s00894-007-0233-4
[41] N.M. O'Boyle, M. Banck, C.A. James, C. Morley, T. Vandermeersch, G.R. Hutchison, Open Babel: An open chemical toolbox, J. Cheminform. 3 (2011) 1-14. **DOI**: https://doi.org/10.1186/1758-2946-3-33
[42] O. Trott, A.J. Olson, AutoDock Vina: improving the speed and accuracy of docking with a new scoring function, efficient optimization, and multithreading, J. Comput. Chem. 31 (2010) 455-461. **DOI**: https://doi.org/10.1002/jcc.21334
[43] G.M. Morris, R. Huey, W. Lindstrom, M.F. Sanner, R.K. Belew, D.S. Goodsell, A.J. Olson, AutoDock4 and AutoDockTools4: Automated docking with selective receptor flexibility, J. Comput. Chem. 30 (2009) 2785-2791. **DOI**: https://doi.org/10.1002/jcc.21256
[44] A.L. Hopkins, G.M. Keserü, P.D. Leeson, D.C. Rees, C.H. Reynolds, The role of ligand efficiency metrics in drug discovery, Nat. Rev. Drug. Discov. 13 (2014) 105-121. **DOI**: https://doi.org/10.1038/nrd4163
[45] X. Pan, H. Wang, Y. Zhang, X. Wang, C. Li, C. Ji, J.Z. Zhang, AA-score: a new scoring function based on amino acid-specific interaction for molecular docking, J. Chem. Inf. Model. 62 (2022) 2499-2509. **DOI**: https://doi.org/10.1021/acs.jcim.2c00050
[46] C. Spearman, The proof and measurement of association between two things, in: J.J. Jenkins, D.G. Paterson (Eds.), Studies in individual differences: The search for intelligence, Appleton-Century-Crofts, New York, 1961, pp. 45-55. DOI not available.

[47] W.R. Knight, A computer method for calculating Kendall's tau with ungrouped data, J. Am. Stat. Assoc. 61 (1966) 436-439.
DOI: https://doi.org/10.1080/01621459.1966.10480879
[48] A. Lee, K. Lee, D. Kim, Using reverse docking for target identification and its applications for drug discovery, Expert Opin. Drug. Discov. 11 (2016) 707-715.
DOI: https://doi.org/10.1080/17460441.2016.1190706
[49] X. Xu, M. Huang, X. Zou, Docking-based inverse virtual screening: methods, applications, and challenges, Biophys. Rep. 4 (2018) 1-16.
DOI: https://doi.org/10.1007/s41048-017-0045-8
[50] J. Caballero, The latest automated docking technologies for novel drug discovery, Expert Opin. Drug. Discov. 16 (2021) 625-645.
DOI: https://doi.org/10.1080/17460441.2021.1918093